

Influence of edge barriers on vortex dynamics in thin weak-pinning superconducting strips

B. L. T. Plourde* and D. J. Van Harlingen

Department of Physics, University of Illinois at Urbana-Champaign, 1110 West Green Street, Urbana, Illinois 61801

D. Yu. Vodolazov

Department of Physics, Nizhny Novgorod University, Gagarin Avenue 23, 603600, Nizhny Novgorod, Russia

R. Besseling, M. B. S. Hesselberth, and P. H. Kes

Kamerlingh Onnes Laboratorium, Leiden University, P. O. Box 9504, 2300 RA Leiden, The Netherlands

(Received 17 November 2000; published 5 June 2001)

We introduce a type of vortex entry edge barrier which controls the critical current in a perpendicular magnetic field in thin-film weak-pinning superconducting strips. Measurements of the critical current in thin-film amorphous-MoGe strips show a linear decrease with increasing magnetic field strength at low magnetic fields, and a crossover at a well-defined threshold field to an inverse power-law decay that is independent of the strip width. This behavior has not been observed previously due to bulk pinning, which only becomes dominant in our MoGe samples at high magnetic fields. To describe our results, we present calculations of the current distribution in thin superconducting strips with a finite penetration depth and negligible bulk pinning, and show that the measured critical currents in our MoGe samples correspond to a current density at the strip edge which approaches the Ginzburg-Landau depairing limit. Shape variations and defects along the strip edges influence the vortex entry conditions, leading to deviations from the ideal behavior, including offsets in the critical current maximum with respect to zero field.

DOI: 10.1103/PhysRevB.64.014503

PACS number(s): 74.60.Jg, 74.76.-w

Sample edges play an important role in the dynamics of vortices in superconductors. In addition to intervortex forces and bulk pinning at defect sites, which limit vortex flow in uniform superconductors, interactions with the edges of a superconductor can significantly affect vortex transport in finite size superconducting structures and thin-film devices. The vortex screening current distribution is distorted near a surface so that the boundary condition of no normal current flow at the surface is satisfied. This distortion creates a surface barrier, first considered by Bean and Livingston,¹ and delays the entry of vortices until a magnetic field strength which can be much greater than the lower critical field H_{c1} when vortex nucleation in the bulk first becomes energetically favorable. Another type of vortex entry barrier can occur in superconductors with a large demagnetizing factor, such as thin platelet crystals in a perpendicular magnetic field. The associated strong curvature of the field lines at the sample edges results in a broad distribution of the screening currents across the entire top and bottom surfaces of the sample. If the sample is thicker than the penetration depth, then the curved field lines can cause the entry of tilted vortex segments at the sample corners. As the segments penetrate further into the superconductor, the length of the segment increases initially, leading to an energetic barrier against vortex entry. These so-called geometrical barriers have been studied extensively, particularly in wide, thick samples of the type-II superconductors.²⁻⁴

In this paper, we consider a different regime for which the sample thickness is much less than the penetration depth so that the vortices behave essentially as 2D objects. In this thin-film limit, the vortices cannot cut across the sample corners, but the large demagnetizing factor again leads to a broad current distribution across the strip width, while the

vortices still interact with the sample edge via a Bean-Livingston surface barrier mechanism. This hybrid effect, which we call an edge barrier, is particularly important for understanding vortex phenomena in microfabricated thin-film devices, including flux-flow noise processes in superconducting quantum interference device,⁵ vortex transport in weak-pinning channels,⁶⁻⁸ and the realization of asymmetric vortex ratchet devices.⁹ To investigate the effect of the edge barrier on the dynamics of vortices, we have measured the magnetic field dependence of the critical current of patterned thin-film amorphous MoGe strips. The weak bulk pinning of this material ensures that the critical current is dominated by the vortex interactions with the strip edge over a wide range of magnetic field. We observe several distinct regimes of magnetic field dependence which we identify with different vortex distributions within the strip. In order to fit our data quantitatively, we have calculated the current distribution and vortex entry conditions for thin-film strips in which the thin-film (transverse) penetration depth is comparable to the strip width, the regime appropriate for our samples and most relevant for typical thin-film superconductor devices.

Using standard photolithographic processing and Ar ion milling, we fabricated strips ranging in width from 10 to 40 μm from 200 nm thick films of amorphous MoGe. Films were sputter deposited onto silicon substrates and had the following properties: superconducting transition temperature $T_c = 6.5$ K, normal state resistivity $\rho_n = 180 \mu\Omega \text{ cm}$, and critical field slope $dB_{c2}/dT|_{T_c} = 2.8 \text{ T/K}$. The superconducting transition-metal glasses have been studied extensively because of their weak vortex pinning,¹⁰ typically exhibiting bulk critical current densities less than 10^4 A/cm^2 at low magnetic fields, several orders of magnitude lower than most superconducting materials. Because of the short electronic

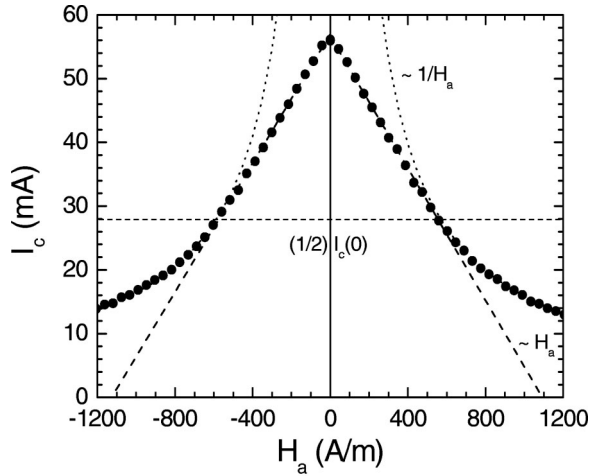


FIG. 1. I_c vs H_a for a 25 μm wide, 200 nm thick a -MoGe strip. Linear fits at low field have slopes of $-51.9 \mu\text{m}$ ($H_a > 0$) and $50.6 \mu\text{m}$ ($H_a < 0$). Curved lines are fits to a_1/H_a , with a_1 equal to $15.9\text{A}^2/\text{m}$ ($H_a > 0$) and $-16.4\text{A}^2/\text{m}$ ($H_a < 0$).

mean free path in these amorphous films, the dirty-limit expressions¹⁰ can be applied, yielding $\lambda(0) = 550$ nm and $\xi_{GL}(0) = 5.1$ nm. Each sample contained four separate strips, each with its own set of wide current leads and a pair of voltage leads separated by 200 μm . During the measurements, the strips were fully immersed in liquid helium for optimum cooling and all the data were obtained at 4.2 K. The Dewar was surrounded by a double-walled μ -metal shield which reduced the residual magnetic flux density at the sample to below 1 mG, and the measurement insert contained a superconducting Helmholtz coil that allowed for the application of uniform magnetic fields up to 2×10^4 A/m (~ 250 Oe). Transport currents were passed through the strips using a custom voltage-controlled current supply, while the voltage along the strip was measured with a low-noise preamplifier coupled to a computer.

We determined the critical current of the strips by slowly increasing the current at a rate of ~ 50 mA/min until the voltage along the strip exceeded the threshold voltage criterion of 1 μV , well above the noise level of our amplifier. Repeated measurements of I_c at zero applied field yielded a variation of less than 0.5 mA for critical currents which were on the order of 50 mA. Changes in the voltage threshold yielded only small variations in the measured value of I_c and did not noticeably modify the field dependence of I_c for low magnetic field. This method provides a better measure of the breakdown of the supercurrent state than the standard technique of extrapolating the flux-flow resistance back to zero voltage to obtain a dynamic critical current, especially at low magnetic field for which the current-voltage characteristics of the strips displayed several knees in the resistive state. These low-field resistive properties of strips with an edge barrier have been studied theoretically,^{11,12} and our measurements of these current-voltage characteristics will be the subject of a future paper.

The field dependence of the critical current, $I_c(H_a)$, for a 25 μm wide, 200 nm thick strip is shown in Fig. 1. As the magnetic field is increased from zero, I_c initially decreases

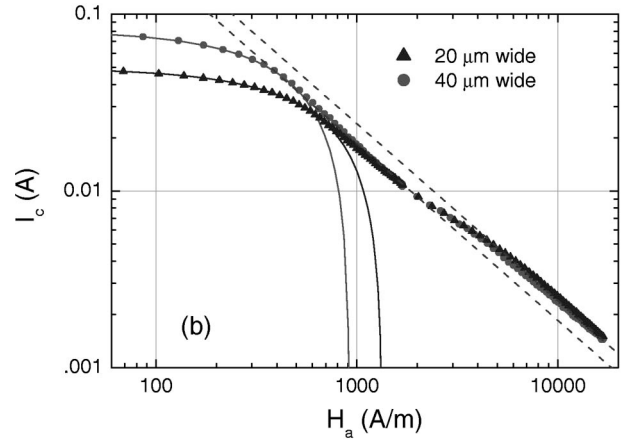
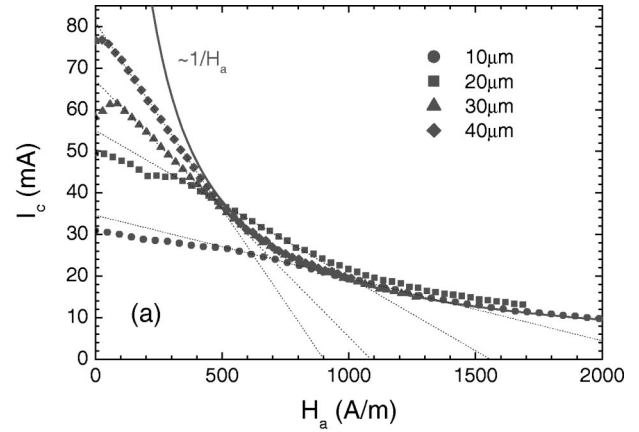


FIG. 2. (a) Linear plot of I_c vs H_a for strips of different widths. All widths merge to a common curve when the critical current drops to 50% of its zero field value. (b) Log-log plot of I_c vs H_a for the 20 and 40 μm wide strips. The curved lines at low fields correspond to the linear fits for the critical current, while the straight dashed lines indicate the two distinct regimes of $1/H_a$ dependence with coefficients a_1 (low field regime) and a_2 (high field regime).

linearly. When I_c drops to approximately one-half of its zero field value, the data deviate from the linear dependence and the critical current decays as H_a^{-1} , as indicated by the curved line. It is significant that the critical current exhibits no hysteresis with magnetic field for fields as large 3500 A/m, indicating the lack of bulk pinning effects on the vortex transport in this range of magnetic field.

We have measured $I_c(H_a)$ for 200 nm thick strips with widths of 10, 20, 25, 30, and 40 μm . All strips show the same qualitative behavior, with wider strips having a larger $I_c(0)$ and a steeper slope dI_c/dH_a for the low-field linear decrease, as shown in Fig. 2(a). The slopes, which are plotted in Fig. 3(a) as a function of strip width, are symmetric with magnetic field polarity to within the uncertainty of the linear fits introduced by errors in the measured I_c . At fields above the linear region, the data merge onto a single curve, indicating that the critical current becomes independent of the strip width. This can also be seen in the double-logarithmic plot in Fig. 2(b) for the 20 and 40 μm wide strips. On this graph, the low-field linear behavior appears as a line with downward curvature that merges into the H_a^{-1} slope. The coeffi-

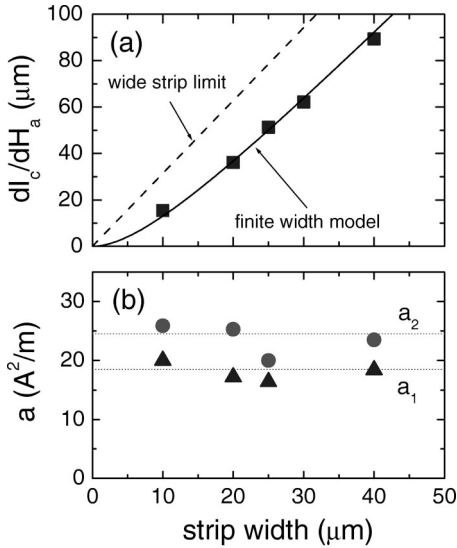


FIG. 3. (a) Low field linear slope vs strip width. Solid line is a fit to our model as described in Eq. (4) with $\lambda = 670$ nm. Dashed straight line has a slope of π and represents the dependence expected from the solution in the wide-strip limit ($W/\lambda_{\perp} \gg 1$). (b) Coefficients a_1 (low field regime) and a_2 (high field regime) of the $1/H_a$ dependence in the intermediate field range vs strip width.

coefficients of the H_a^{-1} fits, a_1 , show no systematic change with the strip width, varying by less than 20%, as shown in Fig. 3(b). This variation is most likely due to different amounts of roughness on the strip edges, thus altering the vortex entry conditions. At somewhat larger magnetic fields, the $I_c(H_a)$ data follow a shallower power-law behavior over a narrow field range that is common for all samples, before again decaying as H_a^{-1} . The coefficients, a_2 , in the high field regime are also independent of strip width but are approximately 15% larger than those in the initial H_a^{-1} region, as shown in Fig. 3(b).

We have also measured the 10, 20, 30, and 40 μm wide, 200 nm thick strips in magnetic fields up to 2.4×10^6 A/m ($\mu_0 H_a \approx 3$ T) in a different cryogenic system with a superconducting solenoid. At these large fields, the actual supercurrent is quite small, while the linear flux-flow slope persists over much of the current-voltage characteristic. Thus in this range of fields, I_c is more appropriately measured by extrapolating the flux-flow resistance back to zero voltage. The critical currents measured at these higher fields continue to vary as H_a^{-1} , although above fields of about 2×10^5 A/m (~ 2.5 kOe), the critical current curves begin to separate such that the wider strips have a larger I_c . For magnetic fields above 2×10^6 A/m, I_c scales linearly with the strip width, thus the critical current density is independent of W and is on the order of 10^2 A/cm 2 for $H_a = 2 \times 10^6$ A/m.

To understand the observed magnetic field dependence of the critical current, we propose a theoretical model for the vortex dynamics in thin-film superconducting strips in which bulk pinning can be neglected. We assume a strip of width W , thickness d , and bulk penetration depth λ , oriented as shown in Fig. 4. The entry and dynamics of vortices in wide, thin superconducting strips for which $W \gg \lambda \gg d$ was studied

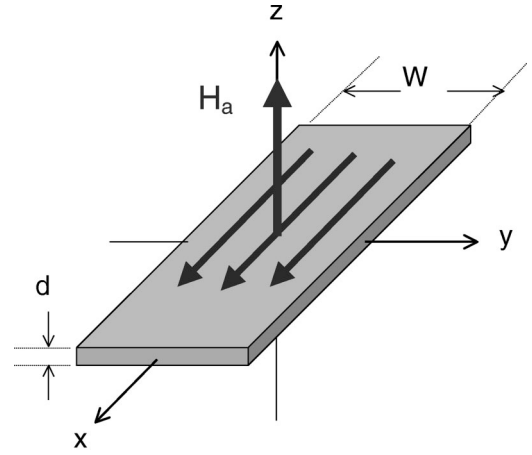


FIG. 4. Schematic of strip layout, defining the axes and parameters used in calculations of the current density distribution.

by Kupriyanov and Likharev,¹³ and more recently extended to strips of moderate thickness ($W \gg d > \lambda$) in which geometrical barriers (due to vortex bending) are important by Benkraouda and Clem.¹⁴ The screening current distribution for wide, thick ($d \gg \lambda$) strips has been studied by Brandt and Mikitik¹⁵ using conformal mapping techniques. In the superconducting strips we have measured, which have dimensions typical for thin-film electronic devices, the thin-film penetration depth $\lambda_{\perp} = \lambda^2/d$ (~ 2 μm for the 200 nm thick films) is comparable to the strip width and hence falls in a regime not previously considered. Although our measured $I_c(H_a)$ curves qualitatively resemble the behavior described by these previous treatments, the finite penetration depth significantly alters the current density distribution across the strip width, which must be determined in order to calculate the conditions for vortex entry. Assuming that the superconducting coherence length $\xi \ll \lambda_{\perp}$, the current density distribution $j(y)$ is given by the Maxwell-London equation^{16,17}

$$\lambda_{\perp} \frac{dj(y)}{dy} + \frac{1}{2\pi} \int_{-W/2}^{W/2} \frac{j(y')}{y-y'} dy' = \left(H_a - \frac{n(y)}{\mu_0} \Phi_0 \right) / d, \quad (1)$$

where H_a is the applied field and $n(y)$ is the spatial density distribution of any magnetic fluxons penetrating the strip.

First we consider the Meissner state of the strip for which $n(y) = 0$. We have solved Eq. (1) numerically in this limit and obtained the following empirical expression for $j(y)$ for an applied field H_a and transport current I that is accurate to $\pm 2\%$ across the width of the strip

$$j(y) \approx \frac{H_a y}{d \sqrt{\alpha [(W/2)^2 - y^2] + \beta \lambda_{\perp} W}} + \frac{I}{2d \gamma \sqrt{(W/2)^2 - y^2 + \delta \lambda_{\perp} W}}, \quad (2)$$

where the fitting parameters α , β , δ and γ are functions of W/λ_{\perp} given by

$$\begin{aligned}
\alpha &= \frac{1}{4} - \frac{0.63}{(W/\lambda_{\perp})^{0.5}} + \frac{1.2}{(W/\lambda_{\perp})^{0.8}}, \\
\beta &= \frac{1}{2\pi} + \frac{\lambda_{\perp}}{W}, \\
\delta &= \frac{2}{\pi} + \frac{8.44}{W/\lambda_{\perp} + 21.45}, \\
\gamma &= \arcsin \frac{1}{\sqrt{1 + 4\delta \frac{\lambda_{\perp}}{W}}}. \quad (3)
\end{aligned}$$

For the range of strips we have studied, $W/\lambda_{\perp} \approx 5-20$, the parameters β , δ , and γ obey the scaling relationship $\gamma\sqrt{\beta\delta} = 1/2$ to within 1%, which will ultimately allow us to express the critical currents in terms of the single parameter β with a high degree of accuracy. For $W/\lambda_{\perp} \gg 1$, these parameters approach the values: $\alpha = 1/4$, $\beta = 1/2\pi$, $\delta = 2/\pi$, $\gamma = \pi/2$, and $j(y)$ coincides with the expression obtained previously for the thin-film, wide-strip limit.^{13,14} A screening current distribution with the general form (2) was measured by Indenbom *et al.*¹⁸ in BSCCO crystals with a rectangular cross section in a perpendicular magnetic field using magneto-optical imaging.

In the absence of bulk pinning, the critical current in the Meissner regime is determined by the conditions for vortices to enter the sample at the edges. The vortices are driven by the Lorentz force from the currents flowing in the strip. At the lowest magnetic fields, the vortices traverse the entire width of the strip, resulting in a finite voltage along the strip. Previous numerical simulations and analytical calculations of vortex entry showed that for a uniform, defect-free surface, a row of vortices first enters the superconductor at a critical value of current density j_s that is approximately equal to the Ginzburg-Landau depairing current density $j_{GL} = \Phi_0/3\sqrt{3}\pi\mu_0\xi\lambda^2$.^{12,19} Defects along the strip edge can allow vortex entry at a lower current density.²⁰ The expression for $j(y)$ in Eq. (2) can be used to calculate the current density at the edges of the strip, $y = \pm W/2$. Thus, the first entry of vortices when $j(+W/2) = j_s$ defines the critical current, $I_c(H_a)$, which for the strips we have measured is given by

$$I_c(H_a) = I_c(0) - \frac{W}{2\beta} H_a = I_c(0) \left(1 - \frac{H_a}{H_s}\right), \quad (4)$$

where $I_c(0) = j_s d \sqrt{\lambda_{\perp} W / \beta}$ is the critical current in zero magnetic field, and $H_s = 2j_s d \sqrt{\beta \lambda_{\perp} / W}$ is the field at which vortices enter the strip when $I = 0$, i.e., no applied transport current. In the wide-strip limit, Eq. (4) approaches the previously obtained result, $I_c(H_a) = I_c(0) - \pi W H_a$.^{13,14}

Now we consider the regime in which there is a net density of vortices in the strip. With no transport current, vortices which enter the strip when H_a exceeds H_s at both edges are pushed towards the center of the strip by the Lorentz force from the screening currents. In the absence of bulk pinning, the resulting vortex distribution exhibits a domelike

profile which is symmetric about the center of the strip. No current flows in the dome region, so the screening currents are confined to the vortex-free areas between the dome and the strip edges.^{13,14,21} A transport current, I in the strip has two effects: it lowers the entry field for vortices to enter at one edge of the strip from H_s to $H_s[1 - I/I_c(0)]$, and it creates a Lorentz force that shifts the vortex dome to one side. The critical current is only reached when the dome boundary touches one edge of the strip so that the vortices can exit the strip and the current density at the opposite edge exceeds the critical entry value, j_s so that vortices can enter the strip, resulting in a finite steady state voltage along the strip. Thus, for current flow in the $+x$ direction, the vortex dome at the critical current extends from $y = -W/2$, the edge of the strip, to a point $y = b$ which depends on H_a . In the presence of a vortex dome, $I_c(H_a)$ can be determined by applying Eq. (2) to the vortex-free part of the strip of width $W' = W/2 - b$, through which all the current must flow. Using the conditions $j(-W'/2) = 0$ (at the edge of the dome, $y = b$) and $j(W'/2) = j_s$ (at the strip edge, $y = W/2$), we obtain the width of the vortex-free region and the critical current of the strip

$$\frac{W'}{\lambda_{\perp}} = \left(\frac{j_s d}{2\sqrt{\pi} H_a}\right)^2 + \sqrt{\left(\frac{j_s d}{2\sqrt{\pi} H_a}\right)^4 + \left(\frac{j_s d}{H_a}\right)^2}, \quad (5)$$

$$I_c(H_a) = \frac{I_c^2(0)\beta}{2WH_a} = \frac{I_c(0)H_s}{4H_a} = \frac{(j_s d)^2 \lambda_{\perp}}{2H_a}, \quad (6)$$

valid in the field regime $H_a > H_s/2$ for which there is a vortex dome. As we observe, this expression predicts that the critical current in the vortex dome regime should be independent of the strip width for the samples we have studied. Physically, this phenomenon occurs because the width of the current-carrying region W' (outside the vortex dome) is independent of the strip width. In the wide-strip limit $I_c(H_a) = I_c^2(0)/4\pi WH_a$, the previously obtained result.^{13,14,22}

Our measurements of the MoGe strip critical currents are in good agreement with the predictions of this model. We observe the initial linear suppression of $I_c(H_a)$ with magnetic field, and, at the predicted reduction to 50% of the peak current, we find the expected crossover to a H_a^{-1} dependence of the critical current and its independence from the strip width. Thus, the field-dependent critical current, as in Fig. 1, can be regarded as a phase diagram for the vortex state of the strip, with the triangular region below the linear curves (and their extrapolations) defining the Meissner phase, and the region bordered by the $1/H$ curve and the extrapolation of the low-field linear curve defining the vortex dome phase. To test the quantitative predictions of our model, we compare the width dependence of the low-field linear slope deduced from our measurements of $I_c(H_a)$ in the Meissner state of the strip, plotted in Fig. 3(a), with the prediction of Eq. (4). The solid line fit is given by $|dI_c/dH_a| = W/2\beta$, as predicted from Eq. (4), taking $\lambda(4.2 \text{ K}) = 670 \text{ nm}$. This value of λ is consistent with independent measurements using a two-coil screening technique. For comparison, we also show the de-

TABLE I. Measured zero-field critical currents $I_c(0)$ and values of the vortex entry current density j_s , for strips of different widths. j_{s0} is calculated from the measured $I_c(0)$ using the expression following Eq. (4), while j_{s1} and j_{s2} are determined from the coefficients of the low-field and high-field regimes of the $1/H_a$ dependence in the vortex dome regime described in Eq. (6).

$W(\mu\text{m})$	$I_c(0)(\text{mA})$	$j_{s0}(10^6\text{A}/\text{cm}^2)$	$j_{s1}(10^6\text{A}/\text{cm}^2)$	$j_{s2}(10^6\text{A}/\text{cm}^2)$
10	35.0	2.3	2.1	2.4
20	52.5	2.0	2.0	2.4
25	56.6	1.9	1.9	2.1
30	62.4	1.8		
40	81.6	2.0	2.0	2.3

pendence expected for the wide-strip limit $|dI_c/dH_a|$, which substantially overestimates the low-field linear slope.

We can use our results to determine the magnitude of the vortex entry critical current density j_s at the strip edge. Values calculated from the measured $I_c(0)$ using Eq. (4), are shown in Table I for the different strip widths. These values are between 70 and 90% of $j_{\text{GL}}(4.2\text{K}) = 2.6 \times 10^6 \text{ A}/\text{cm}^2$, determined by assuming a $(1 - T/T_c)^{-1/2}$ variation for ξ_{GL} , as expected from BCS theory. The reduction of j_s below j_{GL} could be caused by defects along the edge or a tapering of the edge profile. Alternatively, j_s can be deduced from measurements in the vortex dome state of the strip. The corresponding values of j_s from our fits to the initial H_a^{-1} variation are also given in Table I and coincide with the values obtained from the low-field linear fits. Above the crossover to the higher field region of H_a^{-1} variation, the corresponding values of j_s are larger. Although the origin of this crossover is not understood, we find that it occurs when W' , the width of the vortex-free region adjacent to the dome, becomes on the order of λ_{\perp} . This suggests that the crossover may arise from a weaker influence of edge defects on j_s , a scenario that could be tested by experiments with controlled edge defect distributions.

The lack of width dependence of I_c for magnetic fields in the vortex dome regime indicates that the vortex transport in these strips is dominated by the edge barrier rather than bulk pinning. A bulk pinning mechanism would cause the critical current to scale with the strip width. At the largest magnetic fields of our measurements, the critical current due to the edge barrier has been reduced to the level of the critical current due to the residual bulk pinning in the strips, causing the I_c curves to separate according to the strip width. We are planning further measurements with much wider strips to investigate the field dependence of the bulk pinning in these films in order fully discriminate between the edge barrier and bulk pinning contributions.

While all of the strips we have measured show the same qualitative behavior, illustrated by Fig. 1, we have observed deviations in some samples, as shown in Fig. 5, which appear to be related to defects along the strip edge. For some of the strips, we observe a slight offset in the maximum of I_c away from zero field as in $I_c(H_a)$ for the 30 μm strip. This offset is not related to the self-field of the current in the leads, as the polarity of the offset in roughly half of the instances we have observed it is of the wrong sign. A rougher edge on one side of the strip could account for this

offset maximum, as the roughness could lower the entry barrier for vortices along that edge. For the magnetic field and transport current polarities corresponding to the entry of vortices parallel to H_a along the cleaner edge, the lower barriers at the rough edge could allow for the entry of antivortices generated by the strip self-field. An increase in H_a would require a larger transport current to bring in these antivortices, hence a larger I_c . Eventually the applied magnetic field would be large enough to favor the entry of positive vortices along the cleaner edge, corresponding to the maximum in

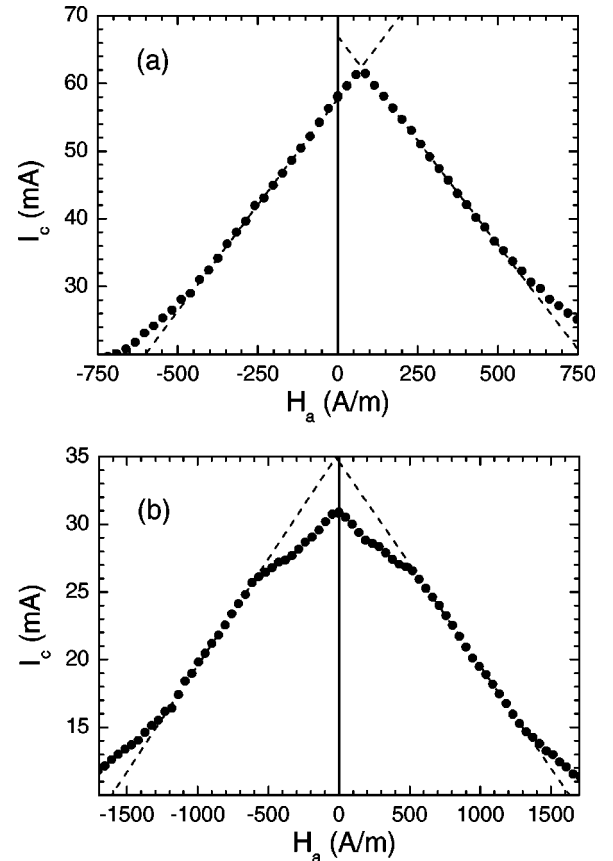


FIG. 5. (a) I_c vs H_a for a 30 μm wide, 200 nm thick a -MoGe strip, exhibiting an offset in the peak critical current, most likely caused by differences in the shape or roughness of the two edges. (b) I_c vs H_a for a 10 μm wide, 200 nm thick a -MoGe strip, showing a reduction of the critical current below the extrapolated linear behavior at small magnetic fields which may be caused by instabilities near defects or non-uniform vortex entry at the edges.

$I_c(H_a)$. Because of the offset maximum observed in some of the strips, $I_c(0)$ is defined as the intersection point of the linear fits for the two polarities of H_a . Some of the strips also exhibit a rounding off of I_c near the zero-field maximum, as in the $I_c(H_a)$ plot for the 10 μm wide strip. This may be related to an instability along the strip edge, possibly localized at edge defects, which causes a breakdown of the supercurrent state for the largest values of the transport current, i.e., near $H_a=0$. Further studies of this effect are planned.

In summary, we have studied the critical current of weak-pinning MoGe thin-film superconducting strips, observing the effects of the edge vortex entry barrier that have previously been masked by bulk pinning. At low magnetic fields, the critical current decreases linearly, determined by when the current density at the edge of the strip approaches the Ginzburg-Landau depairing current density. For larger fields, the critical current decays as an inverse power law and becomes independent of the strip width. At larger magnetic

fields still, the critical current curves separate and eventually scale with the strip width as the residual bulk pinning in the strips dominates the vortex transport. Defects and possible variations of the strip profile along the strip edges reduce the vortex entry conditions below the value expected for a clean edge. Magnetic imaging of the flux entry and dynamics in these strips could address the issues of nonuniformity of the vortex entry.

We would like to thank Brian Yanoff, Kevin Osborn, and Mark Wistrom for technical assistance with the measurements. We have also benefited from useful theoretical discussions with John Clem and Franco Nori. This research was supported by the National Science Foundation through Grant Nos. DMR97-05695 and DMR91-20000, the Science and Technology Center for Superconductivity. We also acknowledge extensive use of the Microfabrication Facilities of the Frederick Seitz Materials Research Laboratory at the University of Illinois.

*Present address: Department of Physics, University of California, Berkeley, CA 94720.

¹C.P. Bean and J.D. Livingston, Phys. Rev. Lett. **12**, 14 (1964).

²E. Zeldov, A.I. Larkin, V.B. Geshkenbein, M. Konczykowski, D. Majer, B. Khaykovich, V.M. Vinokur, and H. Shtrikman, Phys. Rev. Lett. **73**, 1428 (1994).

³R.A. Doyle, S.F.W.R. Rycroft, C.D. Dewhurst, D.T. Fuchs, E. Zeldov, T.B. Doyle, T. Tamegai, S. Ooi, R.H. Drost, P.H. Kes, and D.T. Foord, in *Physics and Materials Science of Vortex States, Flux Pinning and Dynamics*, edited by R. Kossowsky, S. Bose, V. Pan, and Z. Durusoy (Kluwer Academic, Kusadasi, Turkey, 1998), Vol. 356, p. 239.

⁴E.H. Brandt, Phys. Rev. B **59**, 3369 (1999).

⁵D. Koelle, R. Kleiner, F. Ludwig, E. Dantsker, and John Clarke, Rev. Mod. Phys. **71**, 631 (1999).

⁶A. Pruyboom, P.H. Kes, E. van der Drift, and S. Radelaar, Phys. Rev. Lett. **60**, 1430 (1988).

⁷M.H. Theunissen, E.V.d. Drift, and P.H. Kes, Phys. Rev. Lett. **77**, 159 (1996).

⁸R. Besseling, R. Niggebrugge, and P.H. Kes, Phys. Rev. Lett. **82**, 3144 (1999).

⁹J.F. Wambaugh, C. Reichhardt, C.J. Olson, F. Marchesoni, and F.

Nori, Phys. Rev. Lett. **83**, 5106 (1999).

¹⁰P.H. Kes and C.C. Tsuei, Phys. Rev. B **28**, 5126 (1983).

¹¹B.Yu. Blok and S.V. Lempitskii, Fiz. Tverd. Tela **26**, 457 (1984) [Sov. Phys. Solid State **26**, 272 (1984)].

¹²L.G. Aslamazov and S.V. Lempitskii, Zh. Éksp. Teor. Fiz. **84**, 2216 (1983) [Sov. Phys. JETP **57**, 1291 (1983)].

¹³M.Yu. Kupriyanov and K.K. Likharev, Fiz. Tverd. Tela **16**, 2829 (1974) [Sov. Phys. Solid State **16**, 1835 (1975)].

¹⁴M. Benkraouda and J.R. Clem, Phys. Rev. B **58**, 15 103 (1998).

¹⁵E.H. Brandt and G.P. Mikitik, Phys. Rev. Lett. **85**, 4164 (2000).

¹⁶A.I. Larkin and Yu.N. Ovchinnikov, Zh. Éksp. Teor. Fiz. **61**, 1221 (1971) [Sov. Phys. JETP **34**, 651 (1972)].

¹⁷D.Yu. Vodolazov and I.L. Maksimov, Physica C **349**, 125 (2001).

¹⁸M.V. Indenbom, H. Kronmuller, T.W. Li, P.H. Kes, and A.A. Menovsky, Physica C **222**, 203 (1994).

¹⁹D.Yu. Vodolazov, I.L. Maksimov, and E.H. Brandt, Europhys. Lett. **48**, 313 (1999).

²⁰A. Buzdin and M. Daumens, Physica C **294**, 257 (1998).

²¹H. Castro, B. Dutoit, A. Jacquier, M. Baharami, and L. Rinderer, Phys. Rev. B **59**, 596 (1999).

²²L. Burlachkov, A.E. Koshelev, and V.M. Vinokur, Phys. Rev. B **54**, 6750 (1996).